2011 50th IEEE Conference on Decision and Control and
European Control Conference (CDC-ECC)
Orlando, FL, USA, December 12-15, 2011

# A New Longitudinal Flight Path Control with Adaptive Wind Shear Estimation and Compensation

P. Baldi, P. Castaldi, N. Mimmo, A. Torre and S. Simani

*Abstract*— **This paper presents a novel approach to the longitudinal guidance and control issue for an aircraft in presence of wind shear. The main contribution concerns the adaptive estimation of the wind shear disturbances affecting the aircraft and the development of a control scheme suitable to compensate these effects during a precision approach procedure. The work proposes the design, based on the Nonlinear Geometric Approach, of three adaptive filters providing the estimate of the wind shear disturbance components. These estimates are exploited, in an original way, by a BackStepping based controller, thus resulting in an Adaptive BackStepping Controller. Simulation results, obtained by means of a detailed flight simulator implementing the real wind shear condition which caused the 1975 crash of Eastern Flight 066 at JFK airport and a Montecarlo robustness test, demonstrates the effectiveness of the proposed method.**

## I. Introduction

Low–altitude microburst wind shear represents a significant and potentially catastrophic hazard to aircraft taking off or landing. Wind shear consists essentially in a spatial and temporal abrupt change of wind speed and direction. In recent decades, many efforts have been undertaken to develop accurate Wind Shear (WS) models and to develop proper control strategies to face unknown and even severe wind shear situations. These models exploit different wind shear representations modelled through mathematical functions (for example sinusoidal functions) or real data observations.

Until now, robust control methods have been proposed to determine optimal trajectories which allow the aircraft to complete safe abort–landing or take–off procedures [5]–[8]. However, these methods do not permit to complete precision procedures with adequate safety level and desired performance. Again, wind shear estimation methods, based on Extended Kalman Filter (EKF) and Unscented Kalman Filters (EKF/UKF), have been proposed *e.g.* in [9] and [10] respectively.

In this paper a novel approach is proposed. Its goal is to develop a longitudinal guidance and control system which allows the aircraft to follow the glide slope trajectory during a precision approach. The method is focused on the design of three independent Adaptive Filters (AF) providing the estimates of the wind shear disturbance components. These estimates are exploited, in an original way, in a Backstepping based controller, thus resulting in an Adaptive BackStepping (ABS) control scheme, able to compensate wind shear effects. It is worth observing that the AF, whose design is based on the Nonlinear Geometric Approach (NLGA) [3], exploit only attitude and height measures and allow to estimate and compensate wind shear effects in a quick and effective manner.

The paper is organized as follows. Section II provides a brief description of the aircraft longitudinal dynamics model and the WS model used. The WS model is based on an available set of experimental data collected during a real situation. Section III illustrates the application of the NLGA to the AF design. Section IV deals with the design of the ABS control scheme. Section V shows the results achieved in simulation. Concluding remarks are finally presented in Section VI.

## II. Aircraft Dynamic Model

This section provides a brief description of the longitudinal aircraft model considered in this paper. Moreover, the model of the wind shear disturbance is discussed.

### A. Aircraft Equations of Motion

In this study only the longitudinal dynamics is considered. With this assumption, the aircraft equations of motion are defined in the form:

$$\begin{aligned}
\dot{V} &= \tfrac{1}{m}\left[T\cos\alpha - D - mg\sin\gamma - m\left(\dot{W}_x\cos\gamma + \dot{W}_h\sin\gamma\right)\right]\\
\dot{\gamma} &= \tfrac{1}{mV}\left[T\sin\alpha + L - mg\cos\gamma + m\left(\dot{W}_x\sin\gamma - \dot{W}_h\cos\gamma\right)\right]\\
\dot{\alpha} &= q - \dot{\gamma}\\
\dot{q} &= M/I_y
\end{aligned} \tag{1}$$

The elements of the state vector $x = [V, \gamma, \alpha, q]^T$ are the airspeed, the flight path angle, the angle of attack and the pitch rate respectively. The aircraft mass is denoted by $m$. It is worth observing that the aircraft dynamics is affected by the wind shear disturbances through the terms $\dot{W}_x$ and $\dot{W}_h$. The aerodynamic effects are the lift and drag forces, $L$ and $D$, and the pitching moment $M$. These effects can be expressed in term of aerodynamic coefficients as follow:

$$\begin{aligned}
D &= \bar{q}SC_D = \bar{q}S\left(C_{D0} + C_{D\alpha}\alpha + C_{D\delta_e}\delta_e\right)\\
L &= \bar{q}SC_L = \bar{q}S\left(C_{L0} + C_{L\alpha}\alpha + C_{Lq}\hat{q} + C_{L\delta_e}\delta_e\right)\\
M &= \bar{q}S\bar{c}C_m = \bar{q}S\bar{c}\left(C_{m0} + C_{m\alpha}\alpha + C_{mq}\hat{q} + C_{m\delta_e}\delta_e\right)
\end{aligned} \tag{2}$$

where $\bar{q} = \rho V^2/2$ is the dynamic pressure, $\rho$ is the air density, $\hat{q} = q\bar{c}/(2V)$ is the dimensionless pitch rate, $S$ is the wing surface and $\bar{c}$ is the mean aerodynamic chord. Finally, the elements of the input vector $u = [T, \delta_e]^T$ are the thrust and the elevator command respectively.

P. Baldi, P. Castaldi, N. Mimmo, and A. Torre are with the Dipartimento di Elettronica, Informatica e Sistemistica, Università di Bologna, Facoltà di Ingegneria Aerospaziale. Via Fontanelle 40, 47100 Forlì (FC), ITALY (Phone/Fax: +390543786943; e-mail: paolo.castaldi@unibo.it).

S. Simani is with the Dipartimento di Ingegneria, Università di Ferrara. Via Saragat 1E, 44123 Ferrara (FE), ITALY (Phone/Fax: +390532974844; e-mail: silvio.simani@unife.it).

### B. Wind Shear Model

The microburst model is obtained from a reconstruction of the available data referring to the crash of a Boeing 727 occurred on 24 June 1975 at JFK International Airport in New York [1]. The evolution of the wind shear components are shown in Fig. 1. This model of $W_x$ and $W_h$ represents an example of one of the worst conditions that an aircraft may encounter and it represents a valid benchmark to test the validity of the proposed method.

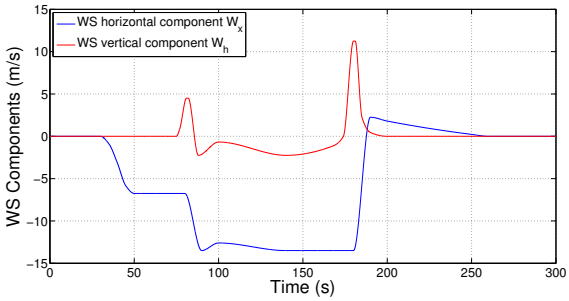


Fig. 1. Wind shear model.

*Remark 1:* For filter design purpose, we assume that the wind shear components can be approximated by their trapezoidal envelops, *i.e.* we assume that their first time derivatives, $\dot{W}_x$ and $\dot{W}_h$, are piecewise constant functions.

## III. Wind Shear Estimation Filter Design

In order to develop an accurate control on the aircraft descent trajectory during an instrumental landing procedure, the estimates of the unknown wind shear disturbance components are necessary. Indeed, these estimates are used to compensate the effects of the wind shear on the aircraft, as shown in Section IV.

This section recalls the design methodology and implementation scheme of the NLGA Adaptive Filters providing the estimates of the disturbance components.

### A. Nonlinear Geometric Approach

The NLGA for Fault Detection and Isolation (FDI) is formally developed in [3]. Its aim is to find, by means of a coordinate change in the state space and in the output space, an observable subsystem that is affected by the fault and not affected by disturbances. Hence, for our purpose, it is assumed that the wind shear disturbance components can be alternatively viewed as faults acting on the system and have to be reciprocally decoupled. More precisely, we need to estimate the wind shear components derivative $\dot{W}_x$ and $\dot{W}_h$, which affects the state dynamics in (1), and the wind shear vertical component $W_h$, which affects the aircraft rate of climb as shown in Section IV.

The proposed approach considers a nonlinear model in the form:

$$\begin{cases} \dot{x} = n(x) + g(x)u + l(x)f + p(x)d \\ y = h(x) \end{cases} \tag{3}$$

in which the state vector $x \in \mathrm{X}$ (an open subset of $\mathbb{R}^{l_n}$), $u(t) \in \mathbb{R}^{l_u}$ is the control input vector, $f(t) \in \mathbb{R}$ is the signal to be estimated (*i.e.* the fault in [3]), $d(t) \in \mathbb{R}^{l_d}$ is the vector embedding the signals which have to be decoupled, and $y \in \mathbb{R}^{l_m}$ is the output vector, whilst $n(x)$, $l(x)$, the columns of $g(x)$ and $p(x)$ are smooth vector fields. Finally, $h(x)$ is a smooth map. Therefore, if $P$ represent the distribution spanned by the column of $p(x)$, the NLGA method can be stated as follows.

First, determine the minimal conditioned invariant distribution containing $P$ (denoted with $\Sigma^P_*$). By using $(\Sigma^P_*)^\perp$ (*i.e.*, the maximal conditioned invariant co–distribution contained in $P^\perp$), determine the largest observability co–distribution contained in $P^\perp$ (denoted with $\Omega^*$). If $l(x) \notin (\Omega^*)^\perp$, the design procedure can continue, otherwise, the fault is not detectable. If this condition is satisfied, it can be found a function $\Phi_1$ and a surjection $\Psi_1$ respectively fulfilling $\Omega^* = span\{d(\Phi_1)\}$ and $\Omega^* \cap span\{dh\} = span\{d(\Psi_1 \circ h)\}$. The functions $\Psi(y)$ and $\Phi(x)$ defined as:

$$\Psi(y) = \begin{pmatrix} \bar{y}_1 \\ \bar{y}_2 \end{pmatrix} = \begin{pmatrix} \Psi_1(y) \\ H_2 y \end{pmatrix} \quad \Phi(x) = \begin{pmatrix} \bar{x}_1 \\ \bar{x}_2 \\ \bar{x}_3 \end{pmatrix} = \begin{pmatrix} \Phi_1(x) \\ H_2 h(x) \\ \Phi_3(x) \end{pmatrix} \tag{4}$$

are (local) diffeomorphisms, where $H_2$ is a selection matrix , $\bar{x}_1 = \Phi_1(x)$ represents the measured part of the state which is affected by $f$ and not affected by $d$, while $\bar{x}_2$ and $\bar{x}_3$ represents the measured and not measured part of the state which are affected by $f$ and $d$. In many cases $\bar{x}_3$ it is not present.

In the new (local) coordinate the so–called $\bar{x}_1$–subsystem written in the form:

$$\begin{cases} \dot{\bar{x}}_1 = n_1(\bar{x}_1, \bar{x}_2) + g_1(\bar{x}_1, \bar{x}_2)u + l_1(\bar{x}_1, \bar{x}_2, \bar{x}_3)f \\ \bar{y}_1 = h(\bar{x}_1) \end{cases} \tag{5}$$

is affected by the single fault $f$ and decoupled from the disturbance vector $d$.

In particular, for the estimation of the two wind shear components derivative $\dot{W}_x$ and $\dot{W}_h$, since the whole state vector is assumed measurable and thus $h(x) = I_4$, it is possible to find two new independent variables. The first $\bar{x}_1$–subsystem is given by the variable $\bar{x}_1 = V\cos\gamma$, which is affected by $f = \dot{W}_x$ and decoupled from $d = \dot{W}_h$; its dynamic equation is:

$$\dot{\bar{x}}_1 = \dot{V}\cos\gamma - V\dot{\gamma}\sin\gamma \tag{6}$$

Again, the second $\bar{x}_1$–subsystem is characterized by the variable $\bar{x}_1 = V\sin\gamma$, which is affected by $f = \dot{W}_h$ and decoupled from $d = \dot{W}_x$; its dynamic equation is:

$$\dot{\bar{x}}_1 = \dot{V}\sin\gamma + V\dot{\gamma}\cos\gamma \tag{7}$$

Finally, the vertical component of the wind shear can be obtained by a numerical integration of its derivative estimation. Clearly, the integrated quantity differs from the true wind shear component $W_h$ by a constant bias. To estimate this bias a further filter can be added to the design. It is based on the following dynamic equation:

$$\dot{\bar{x}}_1 = \dot{H} = V\sin\gamma + W_h \tag{8}$$

Equations (6)–(8), obtained from the exploitation of attitude and height measures, are at the basis of the design of three independent and independently trimmable estimation filters of $W_h$, $\dot{W}_h$ and $\dot{W}_x$.

### B. NLGA Adaptive Filters

With reference to (5), the NLGA Adaptive Filters (NLGA–AF) can be designed if the detectability condition and the following constraints are satisfied [4]:

- the $\bar{x}_1$–subsystem is independent from the $\bar{x}_3$ state components;
- the fault (*i.e.* the wind shear component in this work point of view) is a step function of the time, hence the parameter $f$ is a constant to be estimated;
- there exists a proper scalar component $\bar{x}_{1s}$ of the state vector $\bar{x}_1$ such that the corresponding scalar component of the output vector is $\bar{y}_{1s} = \bar{x}_{1s}$ and the following relation holds:

$$\dot{\bar{y}}_{1s}(t) = M_1(t) \cdot f + M_2(t) \tag{9}$$

with $M_1(t) \neq 0, \forall t \geq 0$. Moreover $M_1(t)$ and $M_2(t)$ can be computed $\forall t$, since they are functions only of input and output measurements.

The relation (9) describes the general form of the system under diagnosis.

Since (6)–(8), with the assumption made in Remark 1, fulfill the above requirements, the design of the AF is achieved, with reference to system model (9), in order to provide a fault estimation $\hat{f}(t)$ which asymptotically converges to the magnitude of the signal (fault) $f$ (in our case the magnitude of $W_h$, $\dot{W}_x$ and $\dot{W}_h$). The proposed adaptive filter is based on a least–squares algorithm with forgetting factor [4]. described by the following adaptation law:

$$\begin{cases} \dot{P} = \beta P - \frac{1}{N^2} P^2 \breve{M}_1^2 & P(0) = P_0 > 0 \\ \dot{\hat{f}} = P \varepsilon \breve{M}_1 & \hat{f}_i(0) = 0 \end{cases} \tag{10}$$

with the following equations representing the output estimation, and the corresponding normalized estimation error:

$$\begin{cases} \hat{\bar{y}}_{1s} = \breve{M}_1 \hat{f} + \breve{M}_2 + \lambda \breve{\bar{y}}_{1s} \\ \varepsilon = \frac{1}{N^2} (\bar{y}_{1s} - \hat{\bar{y}}_{1s}) \end{cases} \tag{11}$$

where all the involved variables are scalar. In particular, $\lambda > 0$ is a parameter related to the bandwidth of the filter, $\beta \geq 0$ is the forgetting factor and $N^2 = 1 + \breve{M}_1^2$ is the normalization factor of the least–squares algorithm.

Moreover, the proposed adaptive filter adopts the signals $\breve{M}_1$, $\breve{M}_2$, $\breve{\bar{y}}_{1s}$ which are obtained by means of a low–pass filtering of the signals $M_1$, $M_2$, $\bar{y}_{1s}$ as follows:

$$\begin{cases} \dot{\breve{M}}_1 = -\lambda \breve{M}_1 + M_1 & \breve{M}_1(0) = 0 \\ \dot{\breve{M}}_2 = -\lambda \breve{M}_2 + M_2 & \breve{M}_2(0) = 0 \\ \dot{\breve{\bar{y}}}_{1s} = -\lambda \breve{\bar{y}}_{1s} + \bar{y}_{1s} & \breve{\bar{y}}_{1s}(0) = 0 \end{cases} \tag{12}$$

Thus, the considered NLGA–AF is described by the systems (10)–(12). Moreover, it can be proved that the adaptive filter provides an estimation $\hat{f}(t)$ that asymptotically converges to the size of $f(t)$. The proofs above can be obtained analogously as shown in [4].

Thus, substituting (1) in (6)–(8), it is possible to make the three dynamics of interest explicit. The first adaptive filter, which is sensitive only to $f = \dot{W}_x$, is based on the following dynamics:

$$\begin{cases} \dot{\bar{y}}_{1s}(t) = M_1(t) \cdot \dot{W}_x + M_2(t) \\ M_1(t) = -1 \\ M_2(t) = \frac{T}{m} [\cos\gamma\cos\alpha - \sin\gamma\sin\alpha] + \\ \qquad - \frac{\bar{q}S}{m} [C_D \cos\gamma + C_L \sin\gamma] \end{cases} \tag{13}$$

The second filter, which is sensitive only to $f = \dot{W}_h$, is based on the following dynamics:

$$\begin{cases} \dot{\bar{y}}_{1s}(t) = M_1(t) \cdot \dot{W}_h + M_2(t) \\ M_1(t) = -1 \\ M_2(t) = \frac{T}{m} [\sin\gamma\cos\alpha + \cos\gamma\sin\alpha] + \\ \qquad - \frac{\bar{q}S}{m} [C_D \sin\gamma - C_L \cos\gamma] - g \end{cases} \tag{14}$$

Finally, the third filter is based on:

$$\begin{cases} \dot{\bar{y}}_{1s}(t) = M_1(t) \cdot W_{hBIAS} + M_2(t) \\ M_1(t) = 1 \\ M_2(t) = V \sin\gamma + \int_0^t \hat{\dot{W}}_h(t)\, dt \end{cases} \tag{15}$$

It is worth observing that the three adaptive filters, based on the dynamics (13)–(15), are completely independent and independently trimmable. Moreover, as previously highlighted, they exploit only attitude and height measures resulting fast and accurate as shown in Section V.

## IV. BackStepping Control Design Scheme

To develop the aircraft longitudinal guidance and control system, we make use of a backstepping based control scheme [11]. The autopilot have to maintain the aircraft on the glide path during a precision approach procedure, even in presence of wind shear. The measure of the distance between the aircraft and the reference trajectory $d$ is precisely computed by the on–board Instrument Landing System (ILS). We also denote the reference path inclination with $\gamma_R$.

Since to follow the reference path the aircraft has to maintain a certain Rate of Climb $RoC = \dot{H} = V \sin\gamma$, it seems appropriate to realize both airspeed and flight path angle control. Thus, we can apply a backstepping procedure as follows. First, the last equation in (1) can be written in the form:

$$\dot{q} = f_q + g_q \delta_e \tag{16}$$

where:

$$\begin{aligned} f_q &= \tfrac{\bar{q}S\bar{c}}{I_y} (C_{m0} + C_{m\alpha}\alpha + C_{mq}\hat{q}) \\ g_q &= \tfrac{\bar{q}S\bar{c}}{I_y} C_{m\delta_e} \neq 0 \end{aligned} \tag{17}$$

Inverting (16), we obtain the elevator control signal realizing the desired dynamics of the pitch rate $\dot{q}_c$, that is:

$$\delta_e = \frac{1}{C_{m\delta_e}} \left[ -C_{m0} - C_{m\alpha}\alpha - C_{mq}\hat{q} + \dot{q}_c \frac{I_y}{\bar{q}S\bar{c}} \right] \tag{18}$$

In order to proceed with the dynamic inversion algorithm, a simplification of the model is needed. Hence, neglecting

some aerodynamic contribution, we obtain the following synthesis model:

$$\begin{aligned}\dot{V} &= T\frac{\cos\alpha}{m} - \frac{\bar{q}S}{m}(C_{D0}+C_{D\alpha}\alpha) - g\sin\gamma \\ \dot{\gamma} &= \frac{1}{V}\left[\frac{T}{m}\sin\alpha + \frac{\bar{q}S}{m}(C_{L0}+C_{L\alpha}\alpha) - g\cos\gamma\right] \\ \dot{\alpha} &= q - \frac{1}{V}\left[\frac{T}{m}\sin\alpha + \frac{\bar{q}S}{m}(C_{L0}+C_{L\alpha}\alpha + C_{Lq}\hat{q}) - g\cos\gamma\right]\end{aligned} \tag{19}$$

Finally, from (19), we obtain the backstepping control signals as follows:

$$q_c = \dot{\alpha}_c + \frac{\bar{q}S}{mV}\left(C_{L0}+C_{L\alpha}\alpha+C_{Lq}\hat{q}\right) + T\frac{\sin\alpha}{mV} - \frac{g\cos\gamma}{V} \tag{20a}$$

$$\alpha_c = \frac{1}{C_{L\alpha}}\left[-C_{L0} + \frac{mV}{\bar{q}S}\left(\dot{\gamma}_c - T\frac{\sin\alpha}{mV} + \frac{g\cos\gamma}{V}\right)\right] \tag{20b}$$

$$T = \frac{1}{\cos\alpha}\left[\bar{q}S(C_{D0}+C_{D\alpha}\alpha) + mg\sin\gamma + m\dot{V}_c\right] \tag{20c}$$

The desired output signals $\dot{y}_c$ in (18) and (20), can be obtained by means of a PI controller, that is:

$$\dot{y}_c = K_p(y_c - y) + K_i\int_0^t (y_c - y)dt \tag{21}$$

where the gain coefficients are determined by applying a linear theory. In Fig. 2 the longitudinal backstepping control scheme is shown.

Thus, it is possible to obtain the input control signals $T(t)$ and $\delta_e(t)$ that allow the aircraft to follow the correct glide path by controlling the two reference input $\gamma_c(t)$ and $V_c(t)$. The signal $V_c(t)$ can be set constant during the descent, while the signal $\gamma_c(t)$ is a function of the aircraft distance from the glide path through the relation:

$$\gamma_c = \arcsin\frac{\dot{d}_c}{V} \tag{22}$$

where, similarly to (21):

$$\dot{d}_c = -K_{pd}d - K_{id}\int_0^t d\,dt \tag{23}$$

In such a way, the control system acts to maintain the aircraft at a zero–distance from the glide path.

At this point, we can consider also wind shear effects, taking into account that the aircraft "true" Rate of Climb (RoC) is affected by the wind shear vertical component $W_h$ as follows:

$$\dot{H} = V\sin\gamma + W_h \tag{24}$$

Solving for $\gamma$ we obtain:

$$\gamma = \arcsin\frac{\dot{H} - W_h}{V} \tag{25}$$

or, from a control point of view:

$$\gamma_c = \arcsin\frac{\dot{d}_c - \hat{W}_h}{V} \tag{26}$$

Equation (26) highlights that the reference control signal $\gamma_c(t)$ is obtained by means of two contributions: the first one belong to the so–called glide slope autopilot and make use of the distance measure $d$ provided by the ILS system, whereas the second contribution exploits the estimate $\hat{W}_h(t)$ provided by the adaptive filter, in order to compensate wind shear effects in real–time.

Moreover, for further performance improvements, the desired output signals $\dot{V}_c$, $\dot{\gamma}_c$ and $\dot{\alpha}_c$ can be corrected through the feedback of the wind shear derivative estimates $\hat{\dot{W}}_x(t)$ and $\hat{\dot{W}}_h(t)$. By defining:

$$\begin{aligned}\hat{u}_V &= -\hat{\dot{W}}_x\cos\gamma - \hat{\dot{W}}_h\sin\gamma \\ \hat{u}_\gamma &= \frac{1}{V}\left(\hat{\dot{W}}_x\sin\gamma - \hat{\dot{W}}_h\cos\gamma\right) \\ \hat{u}_\alpha &= -\hat{u}_\gamma\end{aligned} \tag{27}$$

we obtain the final formulation for the desired output signals as follows:

$$\begin{aligned}\dot{V}_c &= K_{pV}(V_c - V) + K_{iV}\textstyle\int_0^t (V_c - V)\,dt - \hat{u}_V \\ \dot{\gamma}_c &= K_{p\gamma}(\gamma_c - \gamma) + K_{i\gamma}\textstyle\int_0^t (\gamma_c - \gamma)\,dt + \hat{u}_\gamma \\ \dot{\alpha}_c &= K_{p\alpha}(\alpha_c - \alpha) + K_{i\alpha}\textstyle\int_0^t (\alpha_c - \alpha)\,dt - \hat{u}_a\end{aligned} \tag{28}$$

Fig. 2 clearly shows how the estimates provided by the AF are used as feedback in the overall system.

## V. Simulation Results

In order to test the performances brought by the application of the proposed estimation and control scheme, a RQ–2 Pioneer UAV simulator is used.

TABLE I
SIMULATION PARAMETERS

| | |
|---|---|
| $m = 190.512$ [kg] | $C_{D0} = 0.060$ |
| $I_y = 90.948$ [kg m$^2$] | $C_{L0} = 0.385$ |
| $S = 2.826$ [m$^2$] | $C_{m0} = 0.194$ |
| $\bar{c} = 0.548$ [m] | $C_{D\alpha} = 0.430$ [rad$^{-1}$] |
| $H_0 = 500$ [m] | $C_{D\delta_e} = 0.018$ [rad$^{-1}$] |
| $\rho = 1.168$ [kg m$^{-3}$] | $C_{L\alpha} = 4.780$ [rad$^{-1}$] |
| $g = 9.779$ [m s$^2$] | $C_{L\delta_e} = 0.410$ [rad$^{-1}$] |
| $V_0 = 35$ [m s$^{-1}$] | $C_{Lq} = 8.050$ [rad$^{-1}$] |
| $\gamma_R = -3$ [deg] | $C_{m\alpha} = -2.120$ [rad$^{-1}$] |
| $T_{max} = 667.230$ [N] | $C_{m\delta_e} = -1.760$ [rad$^{-1}$] |
| $\delta_{e_{max}} = +20$ [deg] | $C_{mq} = -36.600$ [rad$^{-1}$] |
| $\delta_{e_{min}} = -20$ [deg] | $t_{sim} = 300$ [s] |

The geometric and aerodynamic characteristics of the aircraft and the simulation parameters are summarized in Table I, while the following assumptions are made:

- the aircraft mass is constant;
- the air density is constant;
- a first order dynamics has been introduced to simulate the engine response;
- input and output sensors are characterized by Gaussian additive white noises, whose standard deviations can be obtained by values given in Table II.

TABLE II
SIMULATED SENSOR NOISES

| | |
|---|---|
| $3\sigma_V = 1.5$ [m/s] | $3\sigma_\gamma = 1.5$ [deg] |
| $3\sigma_\alpha = 1.0$ [deg] | $3\sigma_q = 1.0$ [deg/s] |
| $3\sigma_H = 1.0$ [m] | $3\sigma_T = 10$ [N] |
| $3\sigma_{\delta_e} = 1.0$ [deg] | |

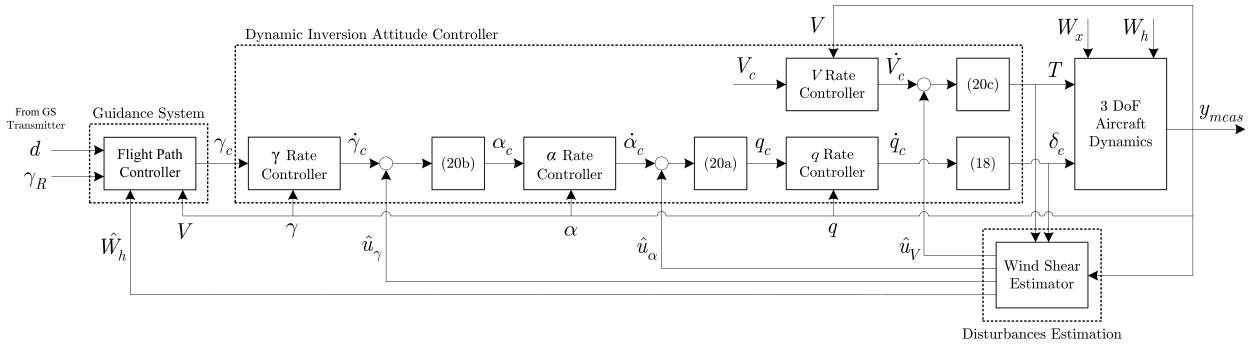


Fig. 2. Longitudinal dynamics controller scheme.

The designed bank of adaptive filters demonstrates to have good transient response and provides asymptotic unbiased estimates $\hat{W}_x(t)$, $\hat{W}_h(t)$ and $\hat{W}_h(t)$. It is worth observing that the estimation filters are robust under working condition (actual wind) that differs from the design assumptions (trapezoidal wind, *i.e.* wind with constant derivative).

As an example, Fig. 3 shows the wind shear vertical component estimate in comparison with its actual values. The estimation error is given in the lower subplot. Similar results were obtained for the wind shear components derivative.

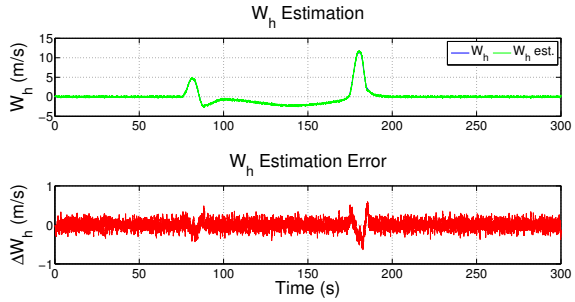


Fig. 3. Comparison of the simulated and estimated wind shear vertical component.

Fig. 4 shows the comparison between the glide path tracking error $d$ for the aircraft provided or not with the wind shear estimates. It is clear how the deviation is higher in the case of a guidance system without the compensation of the wind shear effects, even if the guidance system is capable to restore the right descent trajectory and annihilate the tracking error in any case. Indeed, the maximum tracking error is about 22.5 meters for the guidance system without the wind shear compensation, whilst it is considerably reduced to about 4.5 meters by means the wind shear compensation in the control law.

Fig. 5–7 depicts the evolution of the states $V$, $\gamma$ and $\alpha$, for the controller with and without wind shear compensation. The figures highlight also the differences between the actual output of the system and the measured output. The latter is clearly deteriorated by the simulated sensor noises and affects both the AF estimates (see Fig. 3) and the actual state itself, since it is used for control purpose. It is worth observing that, although the aircraft behavior is completely

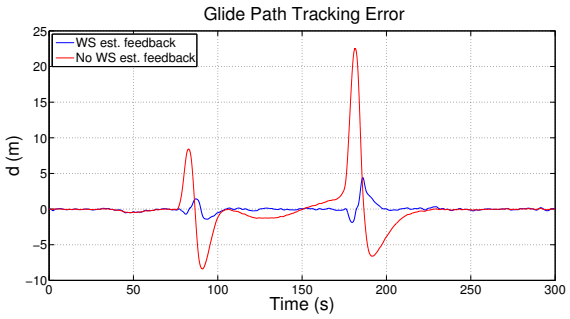


Fig. 4. Aircraft distance (tracking error) from the glide path.

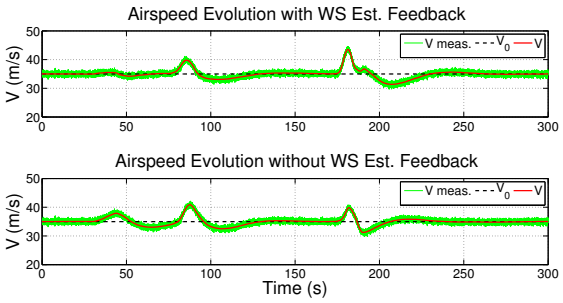


Fig. 5. Comparison of the airspeed evolution, with and without wind shear compensation.

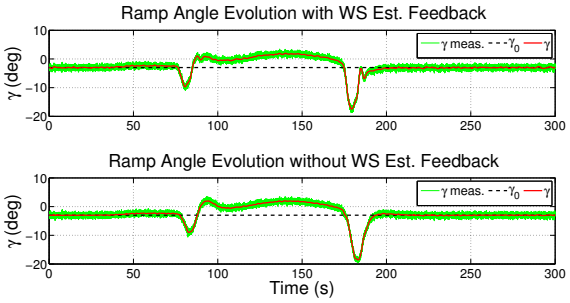


Fig. 6. Comparison of the flight path angle evolution, with and without wind shear compensation.

modified by the wind shear compensation, the control system is able to maintain the state variables within the normal operative range, and with adequate safe margin, in both

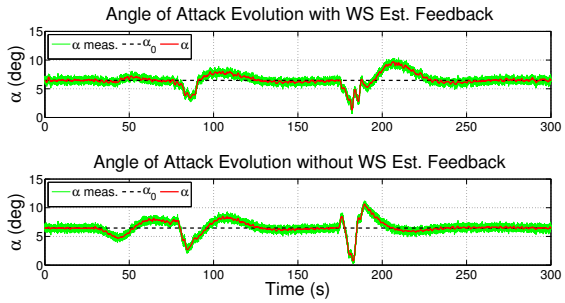


Fig. 7. Comparison of angle of attack evolution, with and without wind shear compensation.

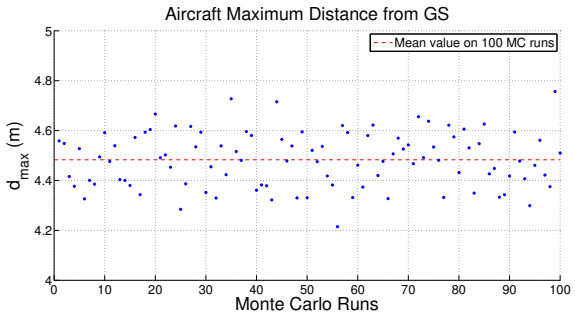


Fig. 8. Maximum glide path tracking error for the uncertain system.

cases. Similar consideration can be done also for the pitch rate, whose evolution is not showed due to a lack of space. As a matter of facts, even though the maneuver is quite aggressive, the angle of attack $\alpha$, for example, never gets larger than approximately $10^\circ$ and the airspeed never drops under 32 m/s. This values are far enough from the stall condition, which is at about $13^\circ$ for an airspeed of 27 m/s. Substantial improvements of the performances are achieved for the whole state vector, thanks to the introduction of wind shear compensation in the control loops.

Moreover, it has been verified that the thrust and the elevator angle values never exceeded the operative limits reported in Table I.

Finally, it can be paid attention to the differences between the actual evolution of the states and the references shown in Fig. 5–7. Indeed, these reference signals refer to the steady condition, that is the windless condition. So, for $t \in [0,30] \cup [260,300]$ s, the whole state vector tracks the reference with zero–error. However, during the windy transient, the aircraft behavior completely matches the control objectives, since the distance from GS is maintained small (see Fig. 4), and reflects the physics of the problem.

### A. Montecarlo Robustness Test

The purpose of this section is to demonstrate, by means of Montecarlo simulations, the robustness of the presented control scheme to parameter uncertainties. The uncertainties are modeled as random variables with uniform distribution. An error in the range $\pm 5\%$ is associated to the aerodynamic coefficients $C_{(\cdot)}$ and the geometric parameters $m$ and $I_y$, whereas the quantities $b$, $\bar{c}$ and $S$ are assumed to be exactly known.

The system has been tested by means of a campaign of 100 Monte Carlo simulations. As an example, Fig. 8 shows the trend of the maximum deviation from the glide path. It can be seen that system performance is weakly deteriorate and the mean deviation from the glide path is approximately equal to the maximum deviation achieved in Fig. 4, which refers to the system without uncertainties.

## VI. Conclusion

This paper presented a novel longitudinal guidance and control system, for an aircraft affected by wind shear disturbances. The main point of the proposed approach consists of developing three independently designed Adaptive Filters (AF), which provide the estimate of the wind shear disturbance components, and their exploiting in a Backstepping control scheme, thus resulting in an Adaptive BackStepping (ABS) control scheme. The AF design is based on the Nonlinear Geometric Approach (NLGA).

Differently from other filtering methods, this approach exploits only attitude and height measures, thus allowing the prompt and effective estimate of the wind shear disturbance components . Thanks to these good wind shear estimates, the controller can thus correct the aircraft behavior in real–time.

Finally, an accurate aircraft model and wind shear data from a simulated actual crash situation showed the effectiveness of the overall guidance and control system in worst case conditions and in presence of model uncertainties.

## References


[1] Donald McLean, "Automatic Flight Control Systems", Prentice Hall International, 1990.

[2] Brian L. Stevens, and Frank L. Lewis, "Aircraft Control and Simulation (2nd ed.)", John Wiley & Sons, 2003.

[3] C. De Persis, A. Isidori, "A geometric approach to nonlinear fault detection and isolation," *IEEE Trans. On Automatic Control*, vol. 6, pp. 853-865, 2001.

[4] P. Castaldi, W. Geri, M. Bonfè, S. Simani, and M. Benini, "Design of residual generators and adaptive filters for the FDI of aircraft model sensors," *Control Engineering Practice*, May 2010, vol.18, Issue 5, pp. 449-459, DOI: doi:10.1016/j.conengprac.2008.11.006.

[5] G. Leitmann, and S. Pandey, "Adaptive control of aircraft in windshear," in *Proc. 30th Conference on Decision and Control*, Brighton, England, December 1991, pp. 2157-2161.

[6] W.Kang, P.K. De, and A. Isidori, "Flight control in a windshear via nonlinear methods," in *Proc. 31st Conf. on Decision and Control*, Tucson, Arizona, December 1992, pp. 1135-1142.

[7] S. H. Pourtakdoust, M. Kiani, and A. Hassanpour, "Optimal trajectory planning for flight through microburst wind shears," *Aerospace Science and Technology*, 2010. Article in Press, DOI:10.1016/j.ast.2010.11.002.

[8] S. S. Mulgund, and R. F. Stengel, "Aircraft flight control in wind shear using partial dynamic inversion," in *Proc. of the 12th American Control Conference*, San Francisco, CA, June 1993, pp. 400-404. Print ISBN: 0-7803-0860-3.

[9] S. S. Mulgund, and R. F. Stengel, "Optimal nonlinear estimation for aircraft flight control in wind shear," in *Automatica*, vol. 32, n. 1, pp. 3-13, 1996.

[10] Yuanwei Jing, Jiahe Xu, Georgi M. Dimirovski, and Yucheng Zhou, "Optimal nonlinear estimation for aircraft flight control in wind shear," in *Proc. of the 28th American Control Conference*, St. Louis, Mo, June 2009, pp. 400-404. Print ISBN: 978-1-4244-4523-3.

[11] J. Farrel, M. Sharma, and M. Polycarpou, "Backstepping-based flight control with adaptive function approximation," in *Journal of Guidance, Control and Dynamics*, vol. 28, n. 6, November-December 2005, pp. 1089-1102, ISSN: 07315090. DOI: 10.2514/1.13030.